Science Arena Publications
Specialty Journal of Electronic and Computer Sciences
ISSN: 2412-7485
Available online at www.sciarena.com
2019, Vol, 5 (3): 10-23

# A Fast Wavelet Packet Transform Based Algorithm for Discrimination of Transformers Magnetizing Inrush Currents from Internal Faults

**Zahra Babaei[1]*, Mohammad Moradi[2]**

[1] Electrical engineering Master, Faculty of Engineering, University of Razi, Kermanshah, Iran.
[2] Assistance Professor, Faculty of Engineering, University of Razi, Kermanshah, Iran.

***Corresponding Author**

***Abstract:*** *Transformers are crucial equipment in a power system, which require reliable solutions for their protection to ensure smooth operation. Identification between internal fault current and inrush current is a challenging problem in the design of transformer protection relay. Current transformer saturation and large inrush currents are the most reported cause of the discrimination algorithms mal-operation. In order to eliminate the impact of the current transformer (CT) saturation on the performance of the proposed technique, the currents are compensated by a CT saturation compensation algorithm in the first step. This paper presents a novel algorithm for power transformer differential protection which differentiates internal faults from magnetizing inrush currents using wavelet packet transform (WPT). The technique is based on pattern recognition of the instantaneous differential currents using wavelet transform. The high-frequency components generated during the disturbance are extracted using a wavelet-based processor stage. In this method, an appropriate criterion at a suitable frequency range is developed. The proposed algorithm is evaluated using various simulated inrush and internal fault current cases on a power transformer that has been modeled using Electromagnetic Transients Program software (EMTP). The results obtained from the proposed technique show good accuracy for discriminating faults in the considered system. In addition, the proposed algorithm uses data of the differential current with a time of quarter cycle under the analysis.*

***Keywords:*** *Differential Protection, Power Transformer, Wavelet Packet Transforms, Internal Fault, Inrush Current.*

## INTRODUCTION

A Power transformer is an essential component in electrical power systems and the relays used for its protection must be reliable, dependable, and should take less operating time. Differential protection is mostly used for the protection of transformer. However, Energisation of the power transformers is the main concern of differential protection. Due to energisation of power transformers, the magnetic core is likely to saturate and draw large magnetizing currents with similar quantities with internal fault currents. Therefore, distinction of inrush current from internal fault is very important in order to improve the reliability and security of differential protection. Many different restrain methods are proposed in recent years.
Since a magnetizing inrush current generally contains a larger second harmonic component, conventional transformer protection systems are designed to restrain during inrush transient phenomenon by sensing second harmonics (Lin et al., 2010; Sykes and Morrison, 1972). The ratio of the second harmonic of

differential current in excess of a preset threshold is interpreted as a present of magnetizing inrush. However, the second harmonic due to CT saturation component may also be generated during internal faults (Liu et al., 1992). Moreover, it was found that in certain cases, the second harmonic generated during internal faults in transformers is relatively large, which impairs the ability of this kind of the criterion. Consequently, the commonly used conventional differential protection technique based on the second harmonic restraint will thus have difficulty in distinguishing between internal fault currents and inrush currents. In (Yabe, 1997), the sum of active power flowing into transformer from each terminal has been considered as a criterion. Because the average power in the inrush current is almost zero, fault current can be discriminated from inrush by large power consumption. The equivalent instantaneous inductance-based technique has been proposed in (Abniki et al., 2010). In this method, it has been shown that the inrush current can be characterized by the drastic variation of the equivalent instantaneous inductance, but this criterion for the fault current is almost constant and therefore, it can be used to distinguish inrush current from faults. In (Shin, Park and Kim, 2003), the fuzzy logic concept has been used to discriminate inrush currents from faults. Some other approaches which use mathematical morphology require a sampling window that is much longer than a cycle (Wu, Li and Wu, 2016). Some artificial neural networks are presented in (Mokryani, Siano and Piccolo, 2010; Ghanizadeh and Gharehpetian, 2014; Balaga, Gupta and Vishwakarma, 2015; Cunxiang and Hao, 2013).

These approaches depend on parameters of the protected transformer. Moreover, they need complex algorithms to carry out the required computations. These algorithms require high number of training patterns.

The frequency analysis can be an effective technique to analyze and classify signals with complex characteristics. The traditional signal processing tools used for frequency analysis are based on the conditions of stationary and periodicity. However, disturbances in power systems are of a non-periodic, non-stationary, short duration and impulse super-imposed nature (Bhasker, Tripathy and Kumar, 2014; Abbas et al., 2016; Aktaibi, Rahman and Razali, 2014; Dashti et al., 2016; Gilles, 2013; Raju, 2011; Atthapol Ngaopitakkula et al., 2014; Jettanasen et al., 2012). Some frequency analysis techniques such as wavelet signal processing algorithm overcome the limitations of the traditional algorithms, e.g. the Fourier based method. Some restrictions are low speed, harmonic pollution, dependence on the parameters of transformer, CT's saturation, large computation burden, large required memory and so on. Hence finding a reliable, fast and proficient approach for discrimination of inrush current from internal fault current is essential.

In this paper, First considering the CT's secondary currents, it is checked whether the CTs are saturated or not. In the case of CT saturation, a compensation algorithm is utilized to compensate the relevant error (Rebizant, Szafran and Wiszniewski, 2011). In the next step, a wavelet-based method is used for discriminating inrush currents from faults. The discrete wavelet transform (DWT) has been applied on the differential currents and different features for inrush currents and faults have been extracted based on wavelet components.

## Proposed algorithm

### Modeled System

To generate the current signals for testing the performance of the proposed algorithm, a power system is modeled using Electromagnetic Transients Program (EMTP). Fig.1 shows the developed model of the considered power transformer connected with the electrical power system. The power system used for the simulation studies is given in Fig.1. Table 1 presents the main parameters for the simulated power transformer.

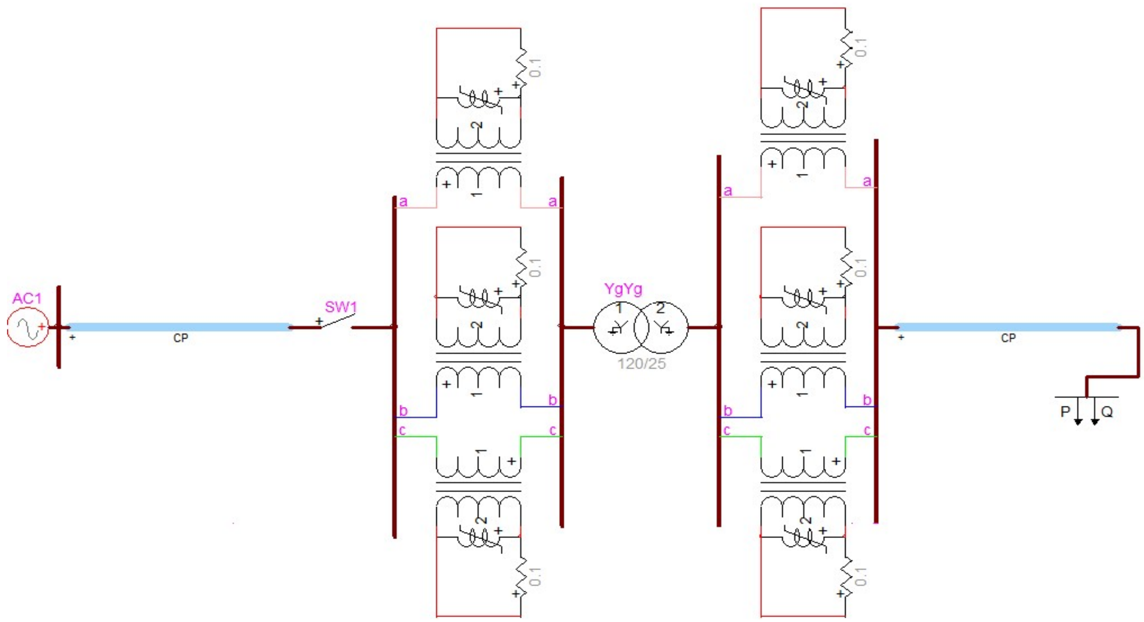


**Figure 1.** Simulated power system model.

**Table 1.** Simulated transformer main parameters.

| | |
|---|---|
| Transformer connection | Yg\Yg |
| Rated power | 47 MVA |
| Voltage ratio | 120\25 KV |
| Rated frequency | 50 Hz |
| Magnetizing reactance | 300 pu |
| Core resistance | 300 pu |
| Primary winding resistance/phase | 0.003 pu |
| Primary winding inductance/phase | 0.09 pu |
| Secondary winding resistance/phase | 0.003 pu |
| Secondary winding inductance/phase | 0.09 pu |

**Effect of CT's saturation**

This part presents an algorithm for the detection and the compensation of the CT saturation condition using the method presented in (Rebizant, Szafran and Wiszniewski, 2011). This method first detects the start of the saturation and then compensates the saturated fragment of the CT's secondary current by using a simple procedure.

- **detection of CT saturation**

An exemplary detailed wave shape of the CT saturated secondary current is shown in Fig. 2, that can be used as illustration and basis for the developed saturation detection methods.

*Procedure of* detect*ion of* CT saturation is based on comparison between the measured secondary current $i_2$ (n) and the estimated secondary current $i_{2e}$(n):

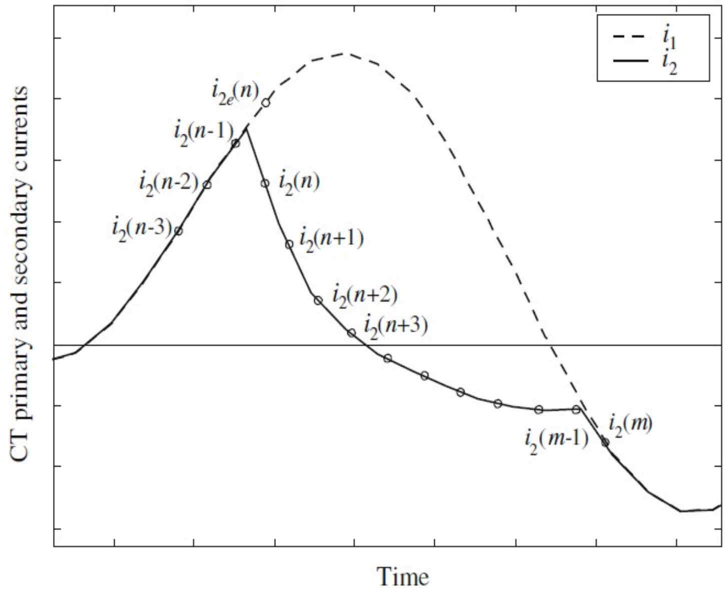


**Figure 2.** CT currents with marked samples before, during and after saturation time.

$|i_{2e}(n) - i_2(n)| \geq \Delta$
&
$|i_{2e}(n)| - |i_2(n)| \geq 0$

If it becomes substantial, it shows that the saturation took place. Otherwise this difference is small and $i_{2e}$ is very close to $i_1$.
$i_{2e}(n)$ may be estimated by the formula:

$i_2(n) \approx 2i_2(n-1) - i_2(n-2)$ (1)
$i_2(n) \approx 3i_2(n-1) - 3i_2(n-2) + i_2(n-3)$ (2)
$i_2(n) \approx 4i_2(n-1) - 6i_2(n-2) + 4i_2(n-3) - i_2(n-4)$ (3)

- **compensation of CT saturation**

Equivalent circuit of the CT reduced to the secondary side is presented in Fig. 3.

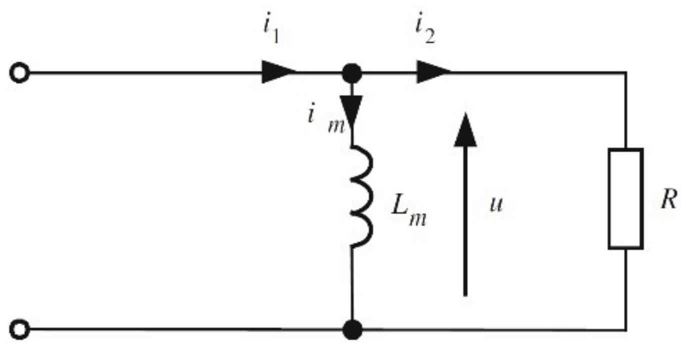


**Figure 3.** Simplified equivalent circuit of the saturated CT.

Estimation of the true values of the secondary current by means of the formula (3) is sufficiently accurate while calculating a maximum of two samples of the current after saturation. Therefore, one may assume that:

$i_{2e}(n) \approx i_1(n)$ $i_{2e}(n+1) \approx i_1(n+1)$

Thus, the samples of the magnetizing current become:

$(n) \approx i_2(n) - i_2(n)$ (4)

$(n + 1) \approx i_2(n + 1) - i_2(n + 1)$ (5)

Then the change of the magnetizing current between the samples (n) and (n + 1) becomes:

$\Delta(n + 1) \approx i_m(n + 1) - i_m(n)$ (6)

The mean value of the CT secondary voltage between the samples (n) and (n + 1) equals:

$$u(n+1) \approx R_2 \frac{i_2(n+1)+i_2(n)}{2} + L_2 \frac{i_2(n+1)-i_2(n)}{T_S} \quad (7)$$

Therefore, the increase of the flux linkage ψ in one sampling period becomes:

$T_s\, u(n+1) \approx \Delta\, \psi(n+1)$ (8)

The value of the magnetizing inductance between the samples is given by the formula:

$$L_m(n+1) \approx \frac{\Delta\, \psi(n+1)}{\Delta\, i_m(n+1)} \quad (9)$$

Now, assuming that between the samples (n + 1) and (n + 2) the magnetizing inductance $L_m$ has the same value, as during the previous sample, one may write:

$$\Delta i_m(n+2) \approx \frac{\Delta\, \psi(n+2)}{L_m(n+1)} \approx \Delta\, i_m(n+1) \frac{\Delta\, \psi(n+2)}{\Delta\, \psi(n+1)} \quad (10)$$

According to formula (6):

$(n + 2) \approx i(n + 1) + \Delta\, i_m(n + 1)$ (11)

The process of calculation of the estimated values of the secondary current samples continues:

$$\Delta\, im(n+k) \approx \Delta\, im(n+k-1) \frac{\Delta\, \psi(n+k)}{\Delta\, \psi(n+k-1)} \quad (12)$$

$i_2(n + k) \approx i_m(n + k) + i_2(n + k)$ (13)

Until the end of the saturated fraction of the period (block scheme of the procedure shown in Fig. 4.

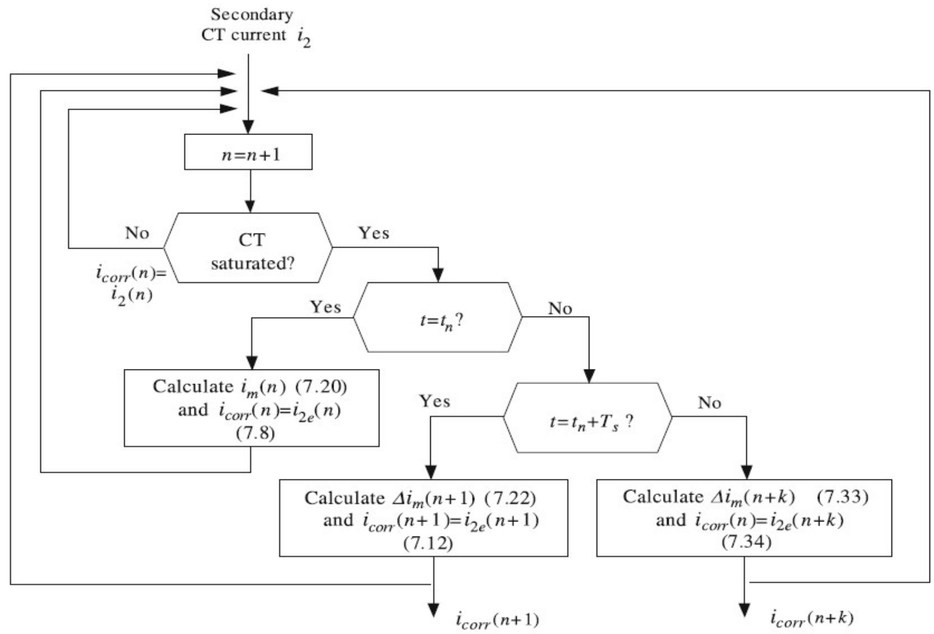


**Figure 4.** Block scheme of the CT saturation correction procedure

- **Simulation results for compensation of CT saturation**

Typical wave shapes of primary and secondary currents in case of a saturated CT with purely resistive burden are presented in Fig. 5.

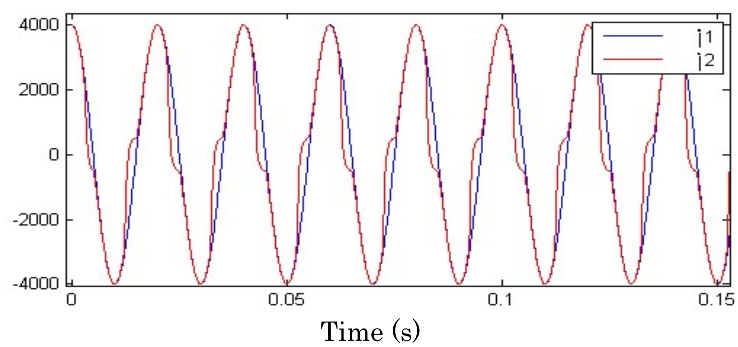


**Figure 5.** Primary and secondary currents for CT saturation time.

Operation of the **CT** correction method presented in 2.2-2 on the secondary current in Fig. 5. are shown in Fig.6.

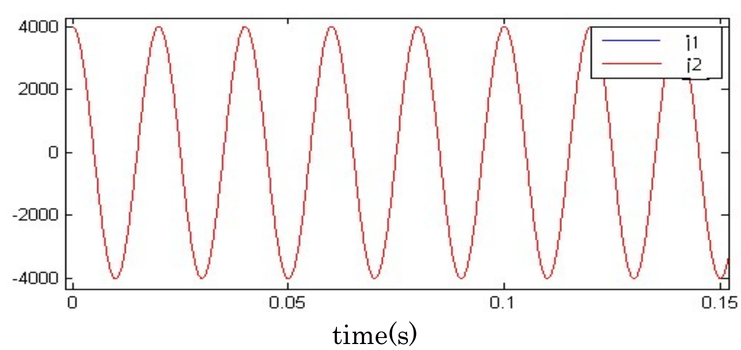


**Figure 6.** Primary and compensated secondary currents.

**Wavelet Transform**

Most of the raw signals in power systems are in time domain whereas distinguished information is hidden in frequency spectrum. Fourier transform (FT) is mostly used to get the frequency information of a stationary signal. FT gives the spectral frequency without any information about where in time those frequencies exist. WT gives good time resolution and poor frequency resolution at high frequencies and good frequency resolution and poor time resolution at low frequencies which makes it suitable for non-stationary signals encountered in power systems. Henceforth wavelet decomposition is ideal for analysing the transient signals and getting much better current characterization and a more reliable discrimination. The wavelet transform can expand signals by using either a shift or a translation time as well as a compression in time or a dilation of a fixed wavelet function referred to as the mother wavelet. Wavelet transform is of three types. Continuous wavelet transform, discrete wavelet transforms and wavelet packet transform.

The wavelet packet is generalized form of the discrete wavelet transform. It decomposes the signal into two bands generated by a tree of low pass and high pass filtering operations (fig.7). The frequency of the box decreases with growing octave number. In other words, with increasing octave number the frequency resolution becomes higher while the resolution is decreased.

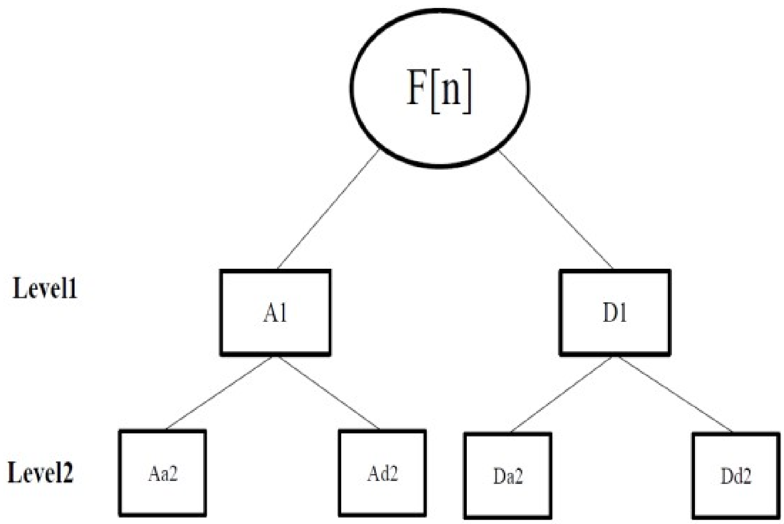


**Figure 7.** two level wavelet packet analysis Approximation details

The wavelet transforms acts as a group of band-pass filters with various central frequencies. It can be zoomed in by scaling and shifting the "mother wavelet". This implies that the wavelet transform can be used to obtain the wanted non-stationary signals and to capture the transient components selectively and accurately. Hence the wavelet transform is an ideal means to extract the different components from the wideband transient signal generated by a fault. Daubechies (db4) mother wavelet with two level of resolution is selected to for the analysis of the signals collected from the transformer model built using EMTP software.

**Discrimination Method**

The results of WPT of different current shows that the magnetizing inrush current have almost low valued coefficients in the second-high level frequency sub band. In this algorithm two levels WPT is implemented and checking for the highest frequency sub band level. The differential current of three phase and corresponding frequency component (Dd2) from WPT due to magnetizing inrush are shown in fig. 8. Switching time is 88.4 ms and residual core flux and phase angle of the supply is chosen BrA =0 and □A = 0 respectively.

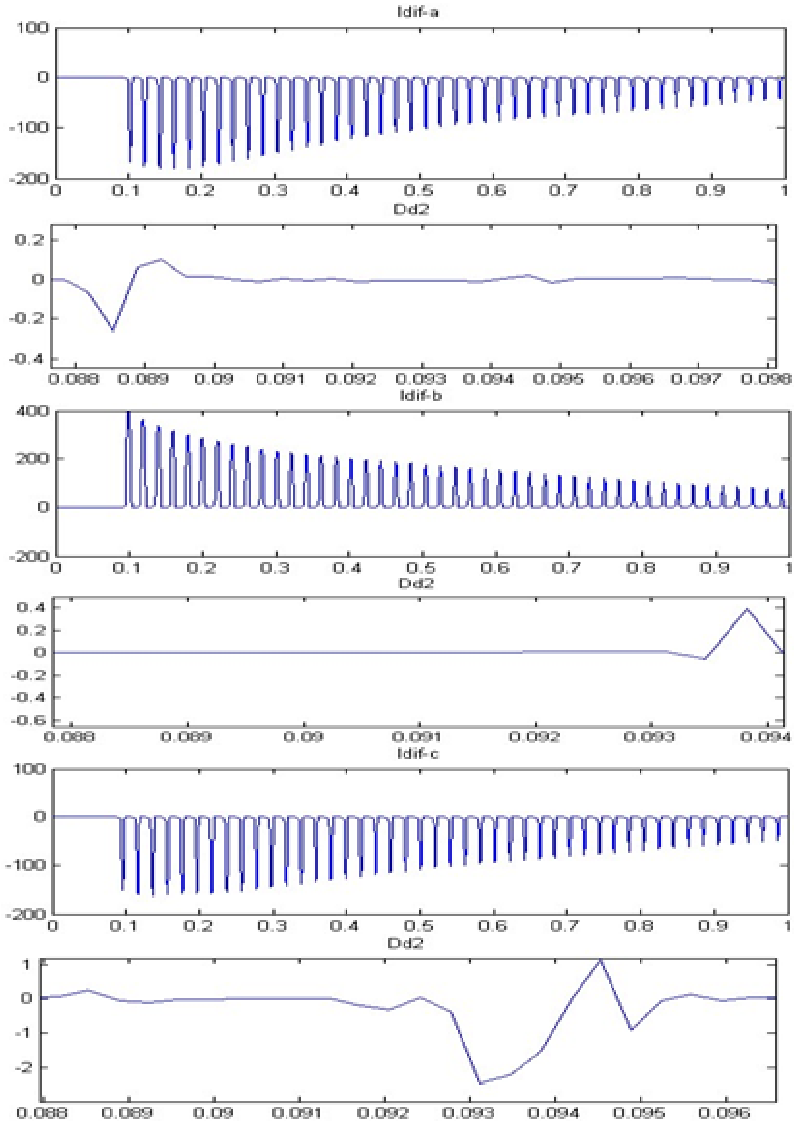


**Figure 8.** Differential current and Frequency range Dd2, inrush

The differential current of three phase and corresponding frequency component (Dd2) from WPT due to (ABC-G) on the secondary side of the transformer is occurred, the transformer is full-load and internal fault at t=92.6 ms occurred, are shown in fig. 9.

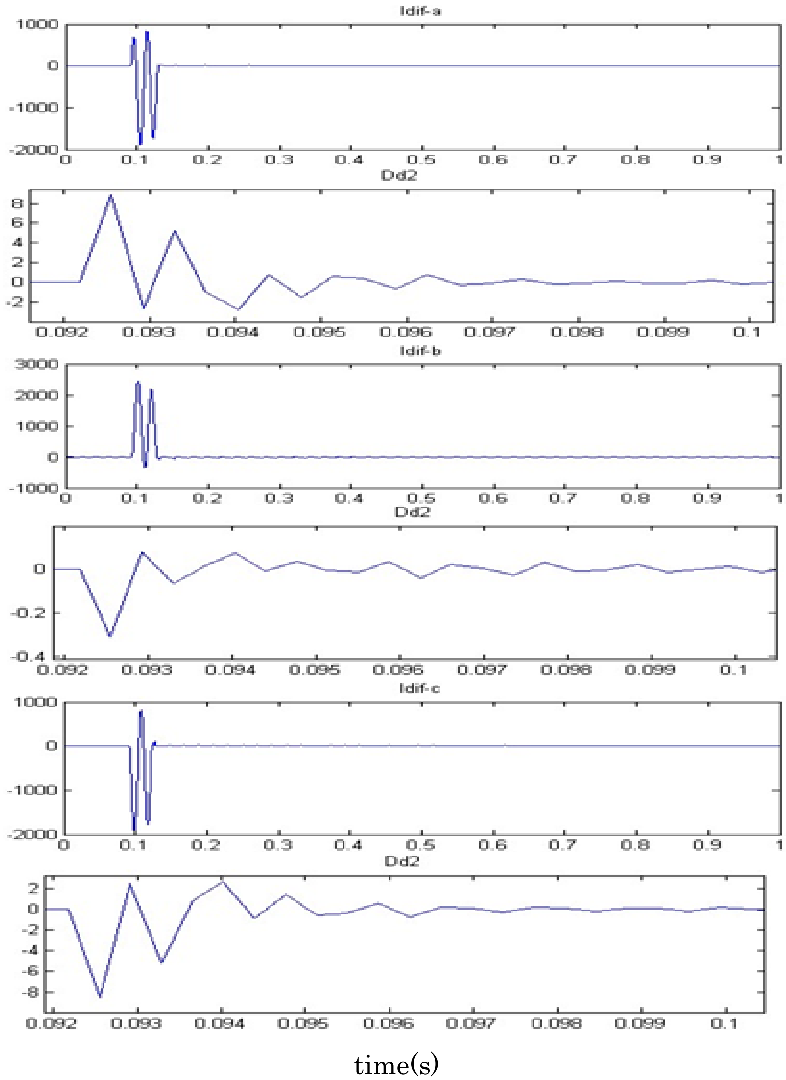


**Figure 9.** Differential currents and Frequency range Dd2, for ABC-G internal fault.

The aforementioned featured are clearly visible in the frequency level Dd2. So, this frequency level has been used as a criterion in the simulations that will be presented. Also, it should be mentioned, with using the absolute value of Dd2, the aforementioned trends can be seen in a better way. So, this value can be used in the algorithms for discrimination of inrush current and faults. Value of the high frequency sub band Dd2 is considered as the diagnosis criterion, and called $am_{max}$. In the case of inrush current, $|am_{max}|$ is lower than a setting ($am_{max} < am_{setting}$), and in the case of internal fault, $|am_{max}|$ is higher than a setting ($am_{max} > am_{setting}$). Comparison of $am_{max}$ with $am_{setting}$ is considered for three phases and if at least in one phase $am_{max} > am_{setting}$, a fault is occurred and the trip command is issued and else, there is no any trip command. The criterion can be used to discriminate the internal fault from the inrush current in about a quarter a cycle. It provides a very quick and simple algorithm.

## Simulation and Result Discussion

### Simulation Results

In order to have a more realistic simulation to verify the validity of the mentioned method in the discrimination of inrush current from fault currents, Internal faults are simulated with different fault inception angles, on-load and no-load conditions and type of fault. Various cases of magnetizing inrush with different percentage of residual core flux, switching-in angle, on-load and no-load conditions that affects differential current are also simulated. Moreover, different cases for simultaneous inrush and fault conditions are simulated.

Fig. 10 shows the three-phase differential currents and the frequency range Dd2 for Idif-a, Idif-b and Idifc,For the case of magnetizing inrush current, the no-load transformer. Switching time is 90 ms and residual core flux and phase angle of the supply is chosen ΦA = 25% and □A=80 respectively. In this figure the frequency range Dd2 in each phase are shown after initiation of disturbance. As it is seen from the Fig. 4 $am_{max}$-a= 0.15, $am_{max}$-b= 2.7 and $am_{max}$-c= 0.57 are obtained.

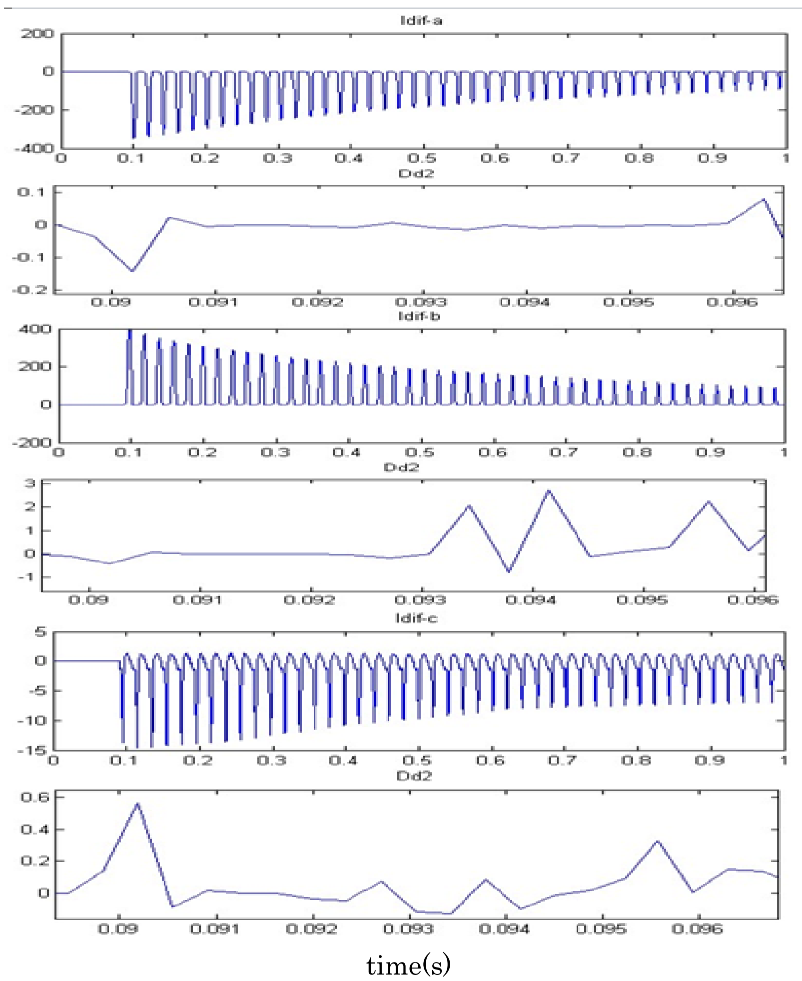


**Figure 10.** Frequency range D2 for Idif-a, Idif-b and Idif –c for unloaded magnetizing inrush.

Investigation of various simulations reveals that values of $|am_{max}|$ for various inrush currents are usually lesser than 3.5 ms. Also for internal fault currents, $|am_{max}|$ is greater than 4.5 ms. Therefore we can choose $am_{setting}$ equal to 4 ms. In this paper $am_{setting}$ is chosen as 4 ms. As seen from Fig. 4 $am_{max}$-a< $am_{setting}$ , $am_{max}$-b< $am_{setting}$ and $am_{max}$-c< $am_{setting}$. Table 2 shows $|am_{max}|$ for Various cases of magnetizing inrush with different percentage of residual core flux, switching-in angle, on-load and no-load conditions that affects differential current. In this table for all of the studied cases, the obtained value of $|am_{max}|$ is lesser than $am_{setting}$. As a result all of these cases are correctly classified as inrush cases.

To obtain the simulation data for internal fault, different faults such as single line-to-ground fault, line-to-line fault, line-to-line-to-ground fault and three phase fault simulated on the inside of the transformer zone. Fig.

11 shows three-phase differential currents and the frequency range Dd2 due to Idif-a, Idif-b and Idif-c, for AB internal fault in excitation unit second winding at time t=97.2 ms, the transformer is noload. As seen from the fig. 5, $am_{max}$-a= 6.07, $am_{max}$-b= 6.15 and $am_{max}$-c= 0.01 are obtained. $am_{max}$-a and $am_{max}$-b which are greater than $am_{setting}$ showing that there is an internal fault and a trip signal will issue.
The table 3 shows $|am_{max}|$ for Various cases of internal faults after disturbance. Simulations have been carried out for different faults in no-load and on-load of power system.

**Table 2.** $am_{max}$ for each phase differential current for inrush

| □A (deg) | phase | No load | | Full load | |
|---|---|---|---|---|---|
| | | ΦA=0 ΦB=0 ΦC=0 | $\Phi_A$=25% $\Phi_B$=25% $\Phi_C$=-50% | ΦA=0 ΦB=0 ΦC=0 | $\Phi_A$=25% $\Phi_B$=25% $\Phi_C$=-50% |
| 30 | a | 0.4 | 0.47 | 0.2 | 0.4 |
| | b | 1 | 1.6 | 0.1 | 0.61 |
| | c | 2 | 3.3 | 2.5 | 2.2 |
| 80 | a | 0.1 | 0.15 | 0.06 | 0.118 |
| | b | 2.17 | 2.7 | 3.1 | 2.18 |
| | c | 0.44 | 0.57 | 0.3 | 0.41 |

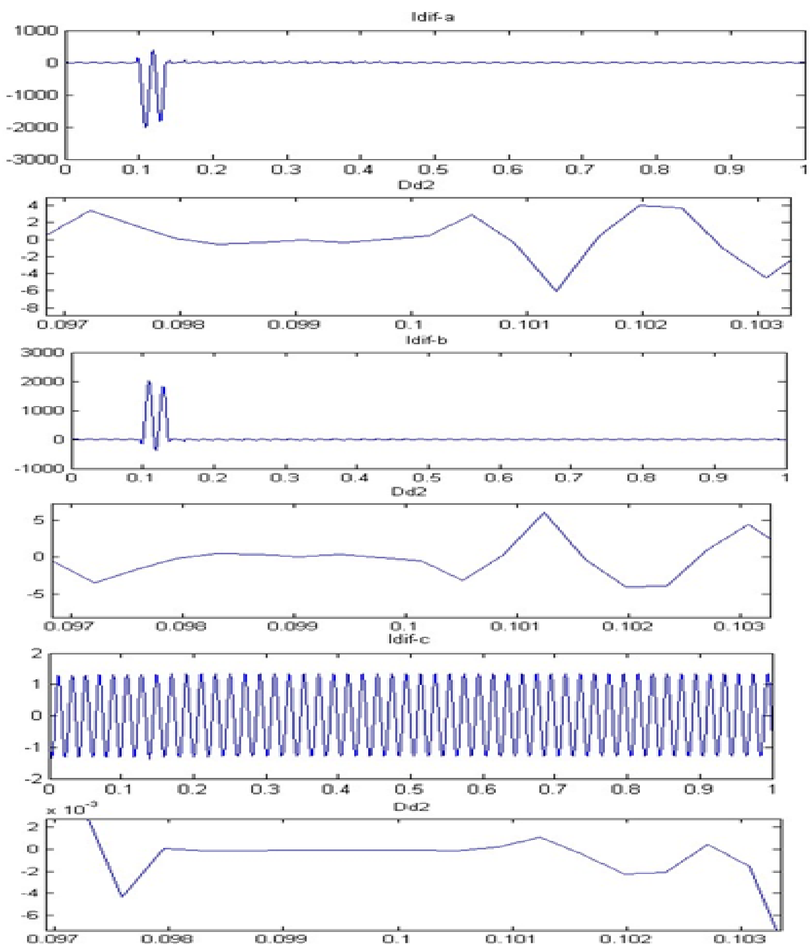


**Figure 11.** Frequency range D2 for Idif-a, Idif-b and Idif-c for AB internal fault.

After studying fault and inrush currents cases separately, simultaneous internal fault and inrush current are considered. Fig. 12 shows the three phase differential currents and Dd2 for Idif-a, Idif-b and Idif-c for simultaneous inrush and fault (AB-G) on the second side at t = 90.6 ms, the transformer is no-load. As seen from the fig. 6, , $am_{max}$-a= 8.67, $am_{max}$-b= 12.31 and $am_{max}$-c= 0.6 are obtained, $am_{max}$-a= 8.67 and $am_{max}$-b= 12.31 which are greater than $am_{setting}$ showing that there is an internal fault and a trip signal will issue.
In Table 4, simultaneous internal fault and inrush current are considered and in all cases the fault has been properly diagnosed fast and reliably.

**Table 3.** $am_{max}$ for internal faults

| phase | No load | | | | Full load | | | |
|---|---|---|---|---|---|---|---|---|
| | a-g | ab | ab-g | abc-g | a-g | ab | ab-g | abc-g |
| a | 6.83 | 6.07 | 3.7 | 3.72 | 7.73 | 4.58 | 7.87 | 8.86 |
| b | 0.1 | 6.15 | 6.82 | 3.11 | 0.05 | 5.45 | 0.1 | 0.31 |
| c | 0.05 | 0.01 | 0.13 | 6.83 | 0.05 | 0.01 | 0.08 | 8.56 |

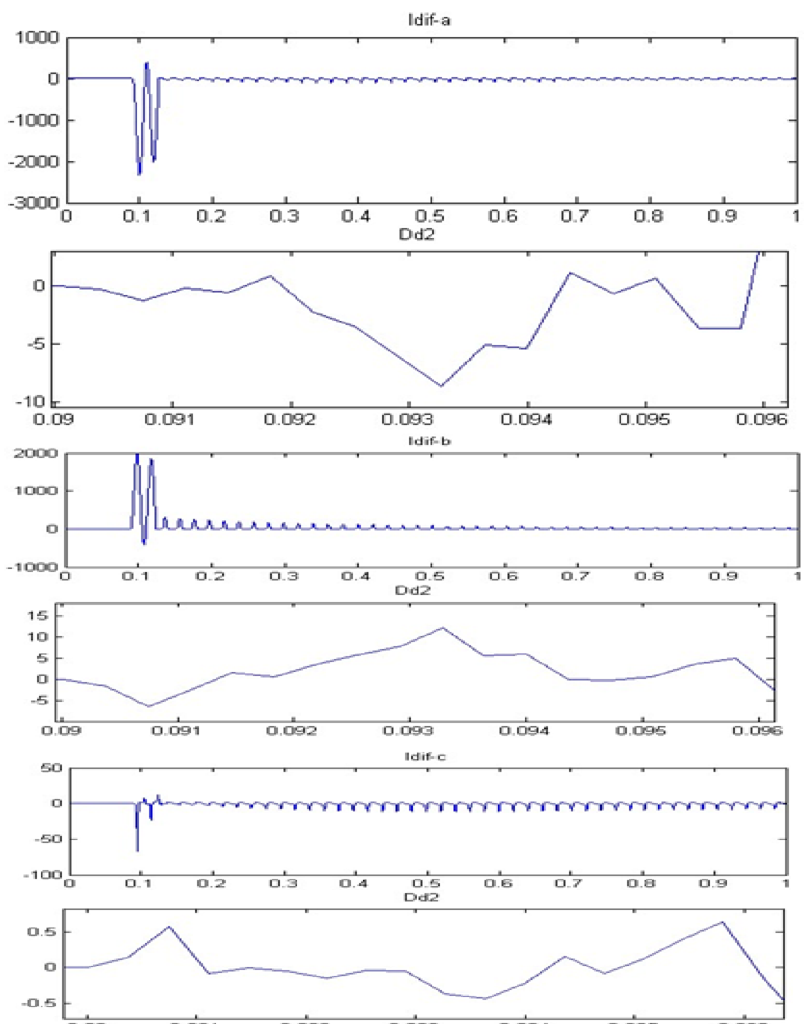


Time (s)

**Figure 12.** Frequency range Dd2 for Idif-a, Idif-b and Idif-c for AB-G internal fault.

**Table 4.** $am_{max}$ for internal faults and inrush current

| □A (deg) | Φr | phase | No load | | | | Full load | | | |
|---|---|---|---|---|---|---|---|---|---|---|
| | | | a-g | a-b | ab-g | abc-g | a-g | a-b | ab-g | abc-g |
| 80 | $\Phi_A$=0 $\Phi_B$=0 $\Phi_C$=0 | a | 6.8 | 5.7 | 1.29 | 1.4 | 6.9 | 5.1 | 1 | 1.43 |
| | | b | 2.43 | 2.79 | 6.45 | 6.58 | 3.74 | 2.72 | 5.72 | 6.58 |
| | | c | 0.43 | 0.42 | 0.43 | 8.02 | 0.2 | 0.3 | 0.3 | 8.01 |
| | $\Phi_A$=25% $\Phi_B$=25% $\Phi_C$=-50% | a | 5.36 | 6.8 | 8.67 | 1.43 | 6.68 | 4.86 | 7.44 | 1.4 |
| | | b | 3.7 | 6.83 | 12.31 | 6.59 | 4.01 | 4.88 | 9.95 | 6.59 |
| | | c | 0.5 | 0.56 | 0.6 | 8.03 | 0.42 | 0.4 | 0.73 | 8.03 |

## CONCLOSION

In this paper, a method based on different behaviors of the differential currents under fault and inrush current conditions has been developed for discriminating of inrush current from fault current in power transformers using wavelet transform. In this algorithm wavelet packet transform based technique is implemented to discriminate the inrush current from internal fault currents of three phase power transformer. The Daubechies (db4) mother wavelet with two number of level of resolution is found to be optimal in providing information to discriminate the inrush currents from internal fault currents of power transformer. Using the developed criterion for three phases, internal faults can be accurately discriminated from inrush currents. To test capabilities of the proposed algorithm, an appropriate power system is modelled with very good accuracy. Many different cases are used for testing the proposed algorithm. The results show that the method can discriminate inrush current from fault current in less than a quarter a cycle based on 50 Hz supply.

## References


1. Abbas, M. F., Zhiyuan, L., Zhiguo, H., & Guanjun, Z. (2016, October). Inrush current discrimination in power transformer differential protection using wavelet packet transform based technique. In 2016 IEEE PES Asia-Pacific Power and Energy Engineering Conference (APPEEC) (pp. 944-948). IEEE.
2. Abniki, H., Monsef, H., Khajavi, P., & Dashti, H. (2010, September). A novel inductance-based technique for discrimination of internal faults from magnetizing inrush currents in power transformers. In 2010 Modern Electric Power Systems (pp. 1-6). IEEE.
3. Aktaibi, A., Rahman, M. A., & Razali, A. M. (2014). An Experimental Implementation of the $ dq $-Axis Wavelet Packet Transform Hybrid Technique for Three-Phase Power Transformer Protection. IEEE Transactions on Industry Applications, 50(4), 2919-2927.
4. Atthapol Ngaopitakkula, Non-member Chaiyan Jettansen, Non-member "A DWT approach to discriminating among Inrush current, External fault, and Internal fault in Power Transformer using Low-Frequency Components Differential current only" IEEJ Trans. 9: 302-314; 2014.
5. Balaga, H., Gupta, N., & Vishwakarma, D. N. (2015). GA trained parallel hidden layered ANN based differential protection of three phase power transformer. International Journal of Electrical Power & Energy Systems, 67, 286-297.
6. Bhasker, S. K., Tripathy, M., & Kumar, V. (2014, July). Wavelet transform based discrimination between inrush and internal fault of indirect symmetrical phase shift transformer. In 2014 IEEE PES General Meeting | Conference & Exposition (pp. 1-5). IEEE.
7. Cunxiang, Y., & Hao, B. (2013, January). The fault diagnosis of transformer Based on the SOM neural network current. In 2013 Fifth International Conference on Measuring Technology and Mechatronics Automation (pp. 1178-1180). IEEE.

8. Dashti, H., Davarpanah, M., Sanaye-Pasand, M., & Lesani, H. (2016). Discriminating transformer large inrush currents from fault currents. International Journal of Electrical Power & Energy Systems, 75, 74-82.
9. Ghanizadeh, A. J., & Gharehpetian, G. B. (2014). ANN and cross-correlation based features for discrimination between electrical and mechanical defects and their localization in transformer winding. IEEE Transactions on Dielectrics and Electrical Insulation, 21(5), 2374-2382.
10. Gilles, J. (2013). Empirical wavelet transform. IEEE transactions on signal processing, 61(16), 3999-4010.
11. Jettanasen, C., Pothisarn, C., Klomjit, J., & Ngaopitakkul, A. (2012, October). Discriminating among inrush current, external fault and internal fault in power transformer using low frequency components comparison of DWT. In 2012 15th International Conference on Electrical Machines and Systems (ICEMS) (pp. 1-6). IEEE.
12. Lin, X., Huang, J., Zeng, L., & Bo, Z. Q. (2010). Analysis of electromagnetic transient and adaptability of second-harmonic restraint based differential protection of UHV power transformer. IEEE Transactions on Power Delivery, 25(4), 2299-2307.
13. Liu, P., Malik, O. P., Chen, D., Hope, G. S., & Guo, Y. (1992). Improved operation of differential protection of power transformers for internal faults. IEEE Transactions on Power Delivery, 7(4), 1912-1919.
14. Mokryani, G., Siano, P., & Piccolo, A. (2010, June). Inrush current detection based on wavelet transform and probabilistic neural network. In SPEEDAM 2010 (pp. 62-67). IEEE.
15. Raju, G. J. (2011). Discrimination between internal faults and inrush currents in power transformers using the wavelet transform. International Journal of Advancements in Technology, 2(2).
16. Rebizant, W., Szafran, J., & Wiszniewski, A. (2011). 'Digital signal processing in power system protection and control' (Springer-Verlag London Ltd,), pp. 98–106.
17. Shin, M. C., Park, C. W., & Kim, J. H. (2003). Fuzzy logic-based relaying for large power transformer protection. IEEE transactions on Power Delivery, 18(3), 718-724.
18. Sykes, J. A., & Morrison, I. F. (1972). A proposed method of harmonic restraint differential protecting of transformers by digital computer. IEEE Transactions on Power Apparatus and Systems, (3), 1266-1272.
19. Wu, W., Ji, T., Li, M., & Wu, Q. (2016). Using mathematical morphology to discriminate between internal fault and inrush current of transformers. IET Generation, Transmission & Distribution, 10(1), 73-80.
20. Yabe, K. (1997). Power differential method for discrimination between fault and magnetizing inrush current in transformers. IEEE Transactions on Power Delivery, 12(3), 1109-1118.